2002033

Mechanisms and Modelling of Cracking under Corrosion and Fretting Fatigue Conditions

Eduardo R. de los Rios
Department of Mechanical Engineering, University of Sheffield, Sheffield, UK

Corrosion Fatigue

It is well established that crack growth proceeds at a higher rate in aggressive environments than in air. This complicates even further the prediction of fatigue life, where safety factors are required to account for these uncertainties. However, considering that these correction factors are derived from projected service conditions (which are shortened in time for laboratory testing), make questionable the accuracy of the predictions, although designs are evaluated through service simulation tests.

To increase the accuracy of the predictions it is necessary to develop models of corrosion fatigue that incorporate the main aspects of the physical phenomena. These aspects of the environmentally assisted corrosion fatigue of metals in aqueous solutions involve electro-chemical processes which include anodic and cathodic reactions. The former is related to an anodic dissolution mechanism and the latter is associated with hydrogen embrittlement. Several possible corrosion fatigue mechanisms related to anodic dissolution have been suggested, including pitting induced crack initiation and short crack growth, film-rupture, dissolution of slip bands at the crack tip and grain boundary oxidation. Of these, pitting corrosion is the most damaging and will be discussed next.

Pitting corrosion

Pitting is the result of electrochemical reactions in local cells on the surface of a metal [1], At the site of a pit, corrosion occurs at the local anode, caused by electrochemical differences between one site and its surrounding area at the metal-liquid interface. Pits are usually found at the origin of fracture in industrial machinery parts as well as on test specimens. This implies that pit initiation triggers fatigue crack initiation. Therefore, the quantitative evaluation of pitting is very important in the prediction of corrosion fatigue life.

Pitting is a common phenomenon occurring above the pitting potential (Ep) for low carbon steel, medium carbon steel and Al-alloys. However, pitting still occurs below Ep in some Al-alloys [2].

In the case of a low stress level and a low loading frequency, pits may play a major role in short fatigue crack initiation and propagation. Akid and Miller [3] observed short fatigue crack initiation at the corner of pits. When pit-depth together with the initiated short crack depth exceeded a critical length, short fatigue cracks propagated at increasing crack growth rates. An example of fatigue cracks initiated at pits is shown in Fig. 1

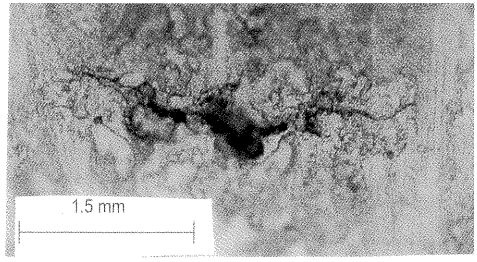

Figure 1. Fatigue crack initiated from a corrosion pit in a high strength steel. Plastic replica after Donohoe [4]

A model of corrosion fatigue was developed by de los Rios et. al [5] which considers the effect of hemispherical pits in the initiation and propagation of fatigue cracks. Experimental evidence has shown that the diameter of the major pit, which eventually created a dominant fatigue crack, increased as a function of time (t), i.e. $t^{1/3}$.

$$H_c - H_o = B(t - t_o)^{1/3} \tag{1}$$

$$H_c - H_o = B[(N - N_o)/f]^{1/3} \tag{2}$$

Where t_o (incubation time), H_c critical pit size, H_o (mean inclusion size) and coefficient B are determined experimentally. Then the number of cycles for pit growth can be calculated as:

$$N_{pit} = f\left(t_o + (H_c - H_o)^3\left(\frac{1}{B}\right)^3\right) \tag{3}$$

Stress concentration around an inclusion or a pit

According to Weiss, Stickler and Blom [6], the field of stress concentration around an isolated micropit was found to extend to approximately twice the radius of the micropit or less. A similar analysis can be used to estimate the effective ranges of stress concentration for a pit. Considering the local pit stress reduces (by a power of the r^{-2} form) for a semi-infinite body, Equation (4) is proposed to evaluate the stress concentration as a function of distance from the pit centre.

$$K_t = (K_{to} - 1)\left(\frac{H_c}{2r}\right)^2 + 1 \qquad (r \geq H_c/2) \tag{4}$$

Consequently, the local stress surrounding the pit, σ_{lc}, as a function of the distance from the original pit centre will take the following form:

$$\sigma_{lc} = \sigma\left[(K_{to} - 1)\left(\frac{H_c}{2r}\right)^2 + 1\right], \; r > H_c / 2 \tag{5}$$

This stress is then used to calculate the number of cycles for crack propagation employing a Paris type crack propagation law, i.e.:

$$\frac{da}{dN} = A(\phi)^n \tag{6}$$

Where ϕ is the crack driving force, e.g. crack tip plastic displacement (CTPD), ΔK, etc. Thus

$$N_{crack} = \int_{a_o}^{a_f} \frac{da}{A(\phi)^n} \tag{7}$$

And total life, for a condition where pit formation is the dominant environmental factor, is:

$$N_T = N_{pit} + N_{crack} \tag{8}$$

Hydrogen embrittlement

For some metals hydrogen embrittlement plays a major role in cathodic reaction-related corrosion fatigue. There are several possible mechanisms put forward to explain hydrogen effects including:(1) a critical hydrogen concentration which induces decohesion, (2) hydrogen environment enhanced crack tip plasticity, (3) corrosion product and roughness induced wake closure, and (4) hydrogen trapping induced intergranular short crack initiation and growth [7,8].

For subcritical fatigue crack propagation, the reversible local plastic flow process may be the dominant mechanism. In the case of hydrogen assisted fatigue crack growth, hydrogen would affect the plastic zone at the crack tip, consequently the effect of hydrogen on the reversible plastic flow has to be considered when applying the crack tip decohesion model. Beachem [9], on the basis of observations made after applying various degrees of deformation to a material degraded by hydrogen (particularly on the lowering of the torsional flow stress in a 1020 steel) proposed a hydrogen assisted cracking theory in which the role of hydrogen is to augment dislocation motion. The 1020 steel case seems to be associated with surface damage [10]. Enhanced dislocation motion by hydrogen is now definitely established, with the extent of the softening being dictated by enhanced screw dislocation mobility, enhanced dislocation injection at surfaces, and the promotion of shear instabilities.

Lynch [11] proposed that some environments including hydrogen, promote crack tip dislocation nucleation and high strain localization in aluminium and iron based alloys. Lankford and Davidson [12] demonstrated that higher crack tip opening strains are responsible for the rapid growth kinetics of small fatigue cracks in aluminium alloys stressed in moist air, at least for cracks in single grains.

It should be emphasized however that the suggestion of a crack tip slip-softening mechanism is based on the observation of hydrogen lowering the yield strength in ductile materials, while for high strength steel, hydrogen has little effect on yield strength, which is controlled by other microstructural features. For lower strength steels ($\sigma_y < 700$ MPa) varying effects have been found. H.Matsui, S.Moriya and H.Kimura [13] found a decrease in yield strength after electrolytic charging at large hydrogen fugacities. Similar results were also reported by Petch [14] for steels with varying carbon content up to 0.60 pct, by Lee et al [15] for spheroidized 1090 steel, by Ciaraldi et at [16] in an Al-Zn-Mg alloy. However, work hardening as opposed to softening has also been observed in many alloys.

Modelling hydrogen-assisted short crack growth

The model of Navarro-de los Rios [17] as extended in [18] was further expanded to incorporate the effect of hydrogen in short fatigue crack growth. The equations which describe the environmental-assisted fatigue process are presented first, and discussed later.
The equilibrium equation of all the forces in the crack system is:

$$\int_{-1}^{l} \frac{f(\zeta')}{\zeta - \zeta'} d\zeta' + \frac{P(\zeta)}{A} = 0 \tag{9}$$

The crack tip open displacement is:

$$CTOD = b \int_{a}^{c} f(\zeta')\, dx \tag{10}$$

The crack growth rate is:

$$\frac{da}{dN} = A\,(CTPD)^{n} \tag{11}$$

The diffusion equation for hydrogen including hydrogen trapping is:

$$\frac{\partial C_L}{\partial t} + \frac{\partial C_T}{\partial t} = D_L \nabla^2 C_L \tag{12}$$

where C_L is the lattice hydrogen concentration, C_T the trapped hydrogen concentration, and D_L the concentration independent lattice diffusivity.

$P(\zeta)$ is a function of hydrogen concentration, $C(x,t)$, which is a complicated time-dependent function, and cannot be expressed in a simple expression. Therefore the integral equilibrium equation (9) has to be solved using the diffusion equation 12. Numerical analyses were carried out on a computer using a one-dimensional explicit differential equation with moving boundary. The moving boundary positions are determined by calculating the crack increment cycle by cycle. Further details of the model are given in reference [19]. Theoretical predictions and the experimental data are compared in Table 1. Because subcritical crack

growth produces a fresh surface after every cycle, it was assumed that the concentration of hydrogen at the crack tip is always equal to the initial concentration C_0 of 0.65 atm ratio.

Table 1. The comparison of the experimental fatigue life with the theoretical predictions for the different stress ranges. Al-Li 8090, frequency = 10 Hz, R = 0.1

	Number of cycles to failure N_f	
Stress range	Experimental data	Prediction
144 MPa	420,900	407,000
	442,000	
180 MPa	219,000	223,000
	183,000	
207 MPa	109,000	115,000
	109,000	

Cracks and hydrogen

It has been believed for sometime, and also proven experimentally [20], that hydrogen induced cracking (HIC) initiation sites correspond to the location of the highest hydrostatic stress σ_h^{max}. However, according to a recent investigation using SIMS (Secondary Ion Mass Spectroscopy) under different ratios of I/II mixed mode loads [21], there are two hydrogen accumulation peaks ahead of the crack tip, i.e. hydrostatic stress induced hydrogen accumulation peak C_H^1 located at the crack tip elastic-plastic boundary and dislocation induced (i.e. plastic strain induced) hydrogen accumulation peak C_H^2 located at the point of highest equivalent plastic strain, which in turn correspond to the point of highest dislocation density very close to the crack tip, see Fig.2.

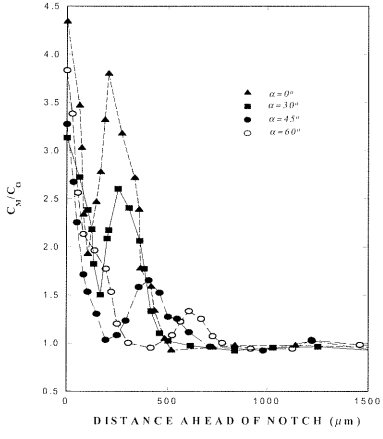

Figure 2. Distribution of Hydrogen concentration ahead of slit (crack)

In terms of these two hydrogen accumulation peaks, the site of hydrogen-induced cracks (HIC) would depend on which peak, in combination with its local maximum normal stress, attains the critical state first. Therefore, for a mode I slit, the hydrostatic stress induced hydrogen accumulation is dominant, and the dislocation induced hydrogen accumulation is rather weak. In this case, the C_H^1 peak plays a more important role than the C_H^2 peak, and consequently the HIC initiation site is determined by the location of the C_H^1 peak (elastic-plastic boundary) Fig. 3(a).

For a combined I/II mode loading case, however, the situation is more complicated since: (i) the HIC initiation sites are at an angle θ with the slit direction and (ii) the HIC initiation site may relate to either C_H^1 or C_H^2 depending on the ratio of K_{II}/K_I as well as on the loading process. Indeed, in slow strain rate (SSR) tests, and when $K_{II}/K_I > 1$, cracks did not form ahead of the notch tip but they initiated at the notch surface where the equivalent plastic strain is maximum (see Fig. 3(b)). Conversely, when $K_{II}/K_I < 1$, HIC initiation did first appear some distance ahead of the slit tip. However, in constant load (CL) tests, the initiation site of HIC is always ahead of the notch tip and associated with the position of the C_H^1 peak as shown in Fig. 3(c).

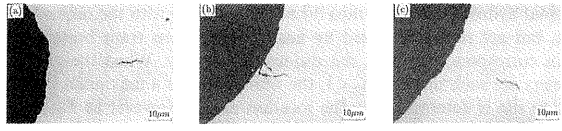

Figure 3. HIC initiation sites at: (a) mode I notch tip; (b) combined I/II mode ($K_{II}/K_I = 3.1$) slit tip (in SSRT tests); (c) combined I/II mode ($K_{II}/K_I = 3.1$) slit tip (in CLT tests).

Fretting Fatigue

Fretting occurs when two surfaces are in contact and subjected to oscillatory tangential movement. The repeated shear stresses that are generated by friction during the relative motion causes surface damage known as fretting wear. Moreover, surface cracks are likely to initiate in the fretting wear zone. This will eventually leads to crack growth and can result in a significant decrease in fatigue life of a material. When fretting damage is associated with decreased fatigue performance, the phenomenon is termed as fretting fatigue. Such a fatigue failure mechanism is extremely common in aircraft structural lap joints and turbine/disk contacts.

Characteristic of fretting fatigue

The mechanism of surface damage that can cause crack nucleation is complex and difficult to study. Surface damage due to wear occurs when the mating surfaces under normal load are

subjected to relative movements. Damage begins with local adhesion between the interface and progresses when adhered particles are removed from the surface. The formation of a fretting scar is typically smaller than a millimetre in depth [22] and they can act as micronotches, raising locally the stress level and providing a site for an emerging fatigue crack.

The general characteristic of fretting fatigue damage is shown in Figure 4.

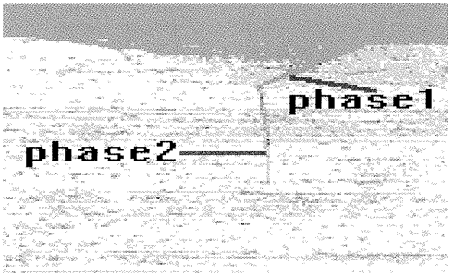

Figure 4. Cross-section of a fretting fatigue crack. Courtesy of R.B. Waterhouse

Fretting fatigue cracks grow initially at a particular angle relative to the surface which depends on the frictional and applied stresses (phase I). As the crack propagates inwards, the contact surface stress decrease. This may lead to crack arrest or if static or alternating stresses exist in the bulk of the material, the crack will change direction and run perpendicular to the surface as a mode I crack. The depth at which this occurs depends on the magnitude of the surface shear stresses, which depend on the coefficient of friction and the normal contact stresses.

Fretting fatigue of aircraft materials: experimental and numerical study

Fretting fatigue cracks in mechanical joints are an ongoing problem in airframes. These cracks initiate under conditions which involve three-dimensional contact stresses between the fastener and panels and between panels themselves. Depending on the fastener system there are several locations where fatigue cracks may initiate. For example, in systems with a low or medium clamping force, the crack initiation site may occur in the minimum net section at the edge of the fastener holes (in the form of a part-elliptical corner crack), or at the intersection of the countersink profile and the hole. Such crack initiation sites lead to a shorter fatigue life of the joint. For fastener systems with high clamping force, the fretting mechanism is dominant and cracks invariably initiate at some distance away from the fastener hole. This crack initiation site results in a substantially increased fatigue life compared to cracks initiated at the minimum net section along a row of rivet holes. Therefore, a comprehensive study of fretting fatigue, with associated modelling, is required for the development of a damage tolerance methodology leading to accurate predictions of fatigue life and thence designs optimisation of high-load transfer joints.

Fretting fatigue experiments

Fretting fatigue tests using Al 2024-T351 specimens and steel and aluminium contact bridge pads, were performed with the axial load amplitude 100 MPa and various values of normal pressure covering the range 10-120 MPa. In all tests fully reversed cyclic axial load was applied with a sinusoidal waveform of 20 Hz frequency. Full details of the experimental set up and test procedure are given in Ref. [23].

The influence of normal load on the fretting fatigue life is shown in Figs. 5 and 6. These figures shows that: (i) there is a considerable reduction in fatigue strength due to fretting; (ii) the fatigue life reduces as the contact pressure increases to a critical value of the normal load; (iii) above this normal load further increase in the normal pressure tends to increase fatigue life.

Shot peening significantly increases the fretting fatigue durability, particularly at low contact stresses. It should be noted that the durability of peened but rough specimens in the medium range of contact pressure is higher than that of polished specimens. This correlates with other work reported in the literature, indicating that there are two beneficial effects of shot peening in fretting fatigue. One is the compressive residual stresses, the other being surface roughness [24]

Aluminium bridges show a similar trend with normal pressure as for steel bridges. However, the critical normal pressure, (giving the shortest life) is achieved with a normal pressure of approximately 40 MPa using aluminium bridges while it is about 80 MPa for steel bridges. Furthermore, fatigue life at normal pressures above the critical point are higher for aluminium bridges than for steel bridges, while the opposite is true below the critical normal pressure for aluminium bridges (see Fig. 6).

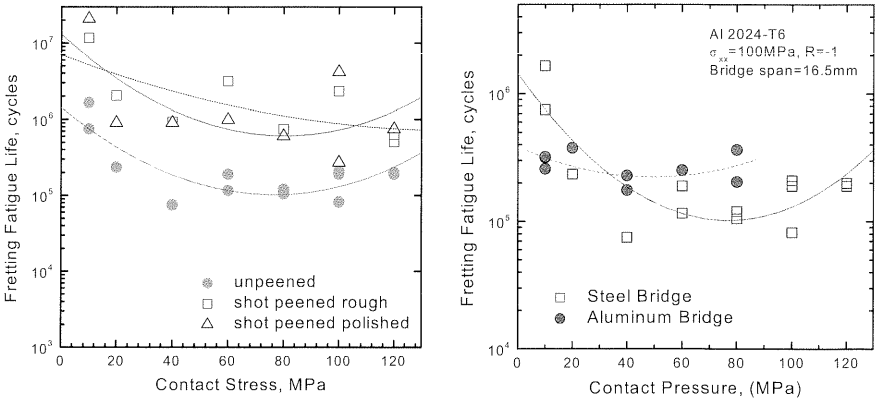

Figures 5 and 6. Fretting fatigue life as a function of contact pressure

Stress Analysis

To predict the initial growth direction and site of fretting fatigue cracks, the fretting damage parameters need to be quantified. To examine the stress distribution on the specimen during cyclic loading, two-dimensional elastic finite element (FE) analysis was carried out under plane strain condition using the commercial finite element package ANSYS. The stress distribution over the contact interface between the specimen and the bridge is shown in Fig. 7.

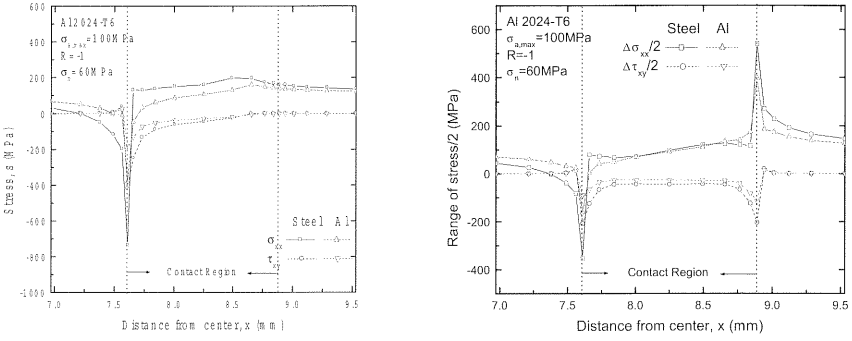

(a) (b)

Figure 7. Stress distribution over the contact area obtained from the numerical analysis

Fig. 7(a) presents the tangential and shear stress distributions along the contact area when the axial cyclic stress achieved its maximum value. It shows that these stresses have peak values at only one of the edges of the pad (leading edge). Fig. 7(b) shows the distribution of the stress ranges during cyclic axial loading. It shows that the range of the tangential and shear stress achieve maximum value at the outer edge of the pad. Comparisons with observations made from the test pieces, confirm this site as being the primary crack initiation location.

From the FE results, the variation of these stresses with angular locations below the leading edges of the bridge feet at various depths, could be investigated. The result of this investigation is summarized in Fig. 8 where the orientation of peak stresses are compared with the initial direction of crack growth obtained from the experiments. It shows that initial crack directions for both contact materials coincide with the direction the maximum value of the tangential stress range, $\Delta\sigma_{\theta\theta,max}$.

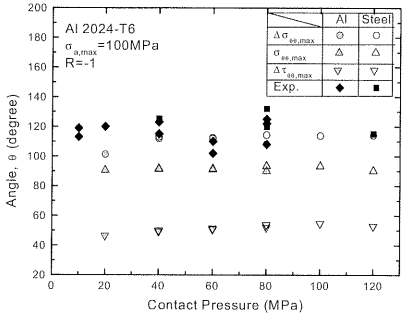

Figure 8. Variation of initial crack growth direction with normal pressure.

Fractographic analysis

The mechanisms of crack initiation and failure are different between peened and unpeened conditions in fretting fatigue. Fig. 9 summarises these differences.

Unpeened specimens **Low contact pressure** The initiation of fretting fatigue cracks in unpeened specimens was always in the form of 3D semi-elliptical surface cracks. At low contact pressure only one crack initiated and propagated to failure	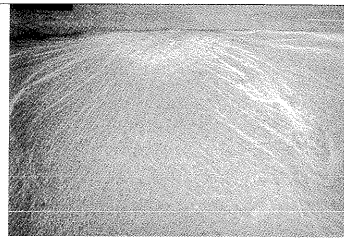
High contact pressure At high contact pressure, on the other hand, there was multicrack initiation which leads to coalescence and to the early formation of a through section crack	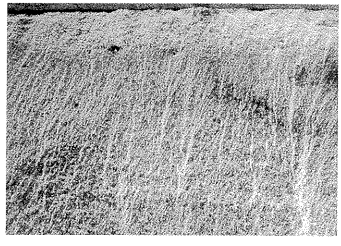

Peened specimens **Low contact pressure** In peened specimens, failure was associated with a single subsurface crack originating from the corner and propagating as a quarter-elliptical crack	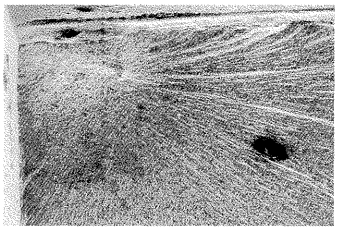
High contact pressure Cracks initiated both at the surface and subsurface. However, all surface cracks were substantially retarded or arrested by the effect of the compressive residual stress left after shot peening 500μm —	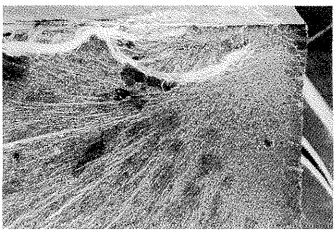

Figure 9. Crack initiation points in fretting fatigue

References

[1] R. H. Brown and R. B. Mears, Ind. Eng. Chem., 33, 1941, 1002.
[2] R. Akid: Ph. D. Thesis, University of Sheffield. UK. 1986.
[3] R. Akid and K. J. Miller, Environment Assisted Fatigue (Ed.: P. Scott, Mechanical Engineering Publications, London, 1990, 415–434.
[4] C. J. Donohoe. Ph.D. Thesis, University of Sheffield 1999.
[5] E. R. de los Rios, X. D. Wu and K. J. Miller. Fatigue Fract. Engng. Mater. Struct. 19, 1383–1400, 1966.
[6] B. Weiss, R. Stickler and A. F. Blom, Short Fatigue Cracks, ESIS 13, (Eds.: K. J. Miller and E. R. de los Rios), Mechanical Engineering Publications, London. 1992, 423–438.
[7] J. P. Hirth, Effects of hydrogen on the properties of iron and steel, Met. Trans. A, vol. 11A, 1980, 861–890.
[8] H. P. Gangloff, and R. P. Wei, Proceedings of the Second Engineering Foundation International Conference, Small Fatigue Cracks, 1986, 239.
[9] C. D. Beachem, Met. Trans., vol. 3, 1972, 437–451.
[10] R. A. Oriani and P. H. Josephic, Acta Met., vol. 22, 1974, 1065–1074.
[11] S. P. Lynch, Metals Forum, vol. 2, 1979, 189–200.
[12] J. Lankford and D. L. Davidson, Fatigue Crack Growth Threshold Concepts, (Eds.: D. Davidson and S. Suresh) Warrendale, PA: TMS-AIME, 1984, 447–463.
[13] H. Matsui, S. Moriya and H. Kimura, Mat. Sci. Eng., vol. 40, 1979, 207–216; Mat. Sci Eng., vol. 40, 1979, 217–225; Mat. Sci. Eng., vol. 40, 1979, 227–234.
[14] N. J. Petch, Phil. Mag., Vol. 1, No. 4, 1956, 331–337.

[15] T. D. Lee, T. Goldenberg, and J. P. Hirth, Met. Trans. A, vol. 10A, 1979, 439; Met Trans. A, vol. 10A, 1979, 199.
[16] S. W. Ciaraldi, J. L. Nelson , R. A. Yeshe and E. N. Pugh, Effect of Hydrogen or Behavior of Materials, (Eds.: I. M. Beinstein and A. W. Thompson), 1980, 437–447.
[17] A. Navarro and E. R. de los Rios (1992), Proc. R. Soc. Lond. A 437, 375–390.
[18] Zuyu Sun, E. R. de los Rios and K. J. Miller (1991), Fatigue Fract. Engng. Mater. Struct., 14, 277–291.
[19] E. R. de los Rios, Zuyu Sun and K. J. Miller (1994), Fatigue Fract. Engng. Mater. Struct., 17, 1459–1474.
[20] R. A. Page and W. W. Gerberich, Metall. Trans. 13A, 1982, 305–311.
[21] Gao Hua, Cao Weijie, Fang Changpeng and E. R. de los Rios, Fatigue Fract. Engng. Mater. Struct. 17, 1994, 1213–1220.
[22] D. A. Hills and D. Nowell, Mechanic of fretting fatigue, Kluwer Academic Publisher, 1994.
[23] U. S Fernando, G. H. Farrahi, and M. W. Brown, Fretting Fatigue, Mechanical Engineering Publications, London, England, 1994, 183–195.
[24] R. B. Waterhouse, Fretting Fatigue, ESIS 18 (Eds.: R. B. Waterhouse and T. C. Lindley), Mechanical Engineering Publications, London, 1994, 339–349.